Chapter 2

In Vitro Techniques for Assessing Neurotoxicity Using Human iPSC-Derived Neuronal Models

Anke M. Tukker, Fiona M. J. Wijnolts, Aart de Groot, Richard W. Wubbolts, and Remco H. S. Westerink

Abstract

The central nervous system consists of a multitude of different neurons and supporting cells that form networks for transmitting neuronal signals. Proper function of the nervous system depends critically on a wide range of highly regulated processes including intracellular calcium homeostasis, neurotransmitter release, and electrical activity. Due to the diversity of cell types and complexity of signaling processes, the (central) nervous system is very vulnerable to toxic insults.

Nowadays, a broad range of approaches and cell models is available to study neurotoxicity. In this chapter we show the applicability of human induced pluripotent stem cell (hiPSC)-derived neuronal co-cultures for in vitro neurotoxicity testing. We demonstrate that immunocytochemistry can be used to visualize networks of cultured cells and to differentiate between different cell types. Live cell imaging and electrophysiology techniques demonstrate that the neuronal networks develop spontaneous activity, including synchronized calcium oscillations that coincide with spontaneous changes in membrane potential as well as spontaneous electrical activity with defined (network) bursting. Importantly, as shown in this chapter, spontaneously active human iPSC-derived neuronal co-cultures are suitable for in vitro neurotoxicity assessment. Future application of live imaging and electrophysiological techniques on hiPSC from different donors and/or patients differentiated in different cell types holds great promise for personalized neurotoxicity assessment and safety screening.

Key words In vitro neurotoxicity screening, Human induced pluripotent stem cell-derived neuronal models, Single-cell fluorescent microscopy, Calcium homeostasis, Membrane potential, Spontaneous neuronal activity, Immunocytochemistry, Multi-well microelectrode array

1 Introduction: Neuronal Network Communication and Neurotoxicity

The (central) nervous system consists of sophisticated neuronal networks that control body function, either via direct control or indirect via input in glands. The main function of neurons that make up the nervous system is to send and receive signals, a process called neurotransmission. To that aim, neurons have a typical structure with dendrites bringing the signal toward the cell body and an axon transmitting the signal away from the cell

Michael Aschner and Lucio Costa (eds.), *Cell Culture Techniques*, Neuromethods, vol. 145,
https://doi.org/10.1007/978-1-4939-9228-7_2,

body. As soon as dendrites receive an excitatory chemical signal, the neuron becomes activated and translates this chemical input signal in an electrical signal, an action potential (AP). Via opening of voltage-gated sodium and potassium channels, the AP induces a change in membrane potential that travels via the cell body along the axon to the synapse at the axon terminal. There, the electrical signal (AP) is converted into a chemical signal that will be transferred to (an)other neuron(s). The first step in conversion from the electrical to the chemical signal involves opening of voltage-gated calcium channels (VGCC), resulting in a strong influx of calcium ions (Ca^{2+}). The resulting changes in the intracellular Ca^{2+} concentration ($[Ca^{2+}]_i$) are involved in a variety of cellular processes such as excitability, plasticity, motility, and viability [1, 2]. $[Ca^{2+}]_i$ is crucial for the regulation of neurotransmission as Ca^{2+} influx through VGCCs triggers the release of neurotransmitters from the presynaptic cell into the synaptic cleft [2–4]. Neurotransmitters are chemical signaling molecules that are stored in vesicles in the presynaptic neuron. There are different types of excitatory and inhibitory neurotransmitters, such as acetylcholine, dopamine, serotonin, glutamate, and gamma-aminobutyric acid (GABA). After release into the synaptic cleft by fusion of the vesicles with the presynaptic plasma membrane, neurotransmitters can bind to receptors on the postsynaptic membrane. In the receiving cell, the signal can then be converted in a new AP, or it can activate intracellular signaling pathways. The chemical signal is terminated by degradation or reuptake of the neurotransmitters from the synaptic cleft (for review see [2, 4]).

Communication in neuronal networks thus critically depends on the structure of neurons, intact neuronal membranes, and regulation of cellular and molecular mechanisms underlying neurotransmission. Additionally, proper neuronal communication also depends on supporting cells such as oligodendrocytes, astrocytes, and microglia. The multicellular nature of the networks can be confirmed with techniques as immunocytochemistry, whereas proper intracellular signaling can be studied with imaging techniques focusing on intracellular calcium levels and the membrane potential. Finally, the resulting network activity can be assessed with the use of multi-well microelectrode arrays (mwMEA).

Its complexity and poor regenerative capacity make the nervous system vulnerable to toxic insults caused by chemical, physiological, and biological agents that are present in the surrounding environment. Neurotoxicity is thus defined as an adverse effect caused by any of these agents on the structure and/or function of the nervous system. Nowadays, there is a broad range of approaches and cell models to study neurotoxicity in vitro.

1.1 Methods to Study Neuronal Network Communication

In vitro cell models should mimic the in vivo situation as closely as possible. For neurotoxicity testing, this means that the in vitro model must form functional neuronal networks with both inhibitory and excitatory neurons as well as supporting cells. In order to circumvent interspecies translation, cells from human origin are the preferred option. Recently, human induced pluripotent stem cell (hiPSC)-derived neurons became commercially available. A benefit of these cells is that they do not require long differentiation into neural progenitor cells and ultimately into functional neurons, which can take several weeks [5, 6] till months [7, 8]. It has been shown that these hiPSC-derived neurons exhibit the behavior and function of mature neurons [7, 8]. Therefore, we chose to use mixed hiPSC-derived neuronal models for the techniques described in this chapter.

First of all, it is important to determine whether the cultured cells form neuronal networks. This can be studied using fluorescent antibodies and confocal microscopy to detect specific target proteins in the cell or on the cell membrane. Besides studying network formation and complexity, immunofluorescent stainings can be used to differentiate between (neuronal) cell types in co-cultures.

Once the cells formed mixed neuronal networks, spontaneous network activity and the effect of toxic insults can be studied by looking at intracellular calcium homeostasis. Changes in $[Ca^{2+}]_i$ can be analyzed by loading the cultured cells with a high-affinity Ca^{2+}-responsive fluorescent dye. Similarly, fluorescent voltage-sensitive dyes can be used to study changes in membrane potential as an indication for the occurrence of electrical activity.

Another way to look at spontaneous neuronal network activity and (network) bursting and toxic effects hereon is by the use of electrophysiological methods. The introduction of mwMEAs provided a way to grow cells on a culture surface with an integrated array of microelectrodes. This allows for simultaneous and noninvasive recording of extracellular local field potentials at a millisecond time scale at different locations in the network grown in vitro (for review see [9]). Mammalian neuronal networks grown in vitro on mwMEA display many characteristics of in vivo neurons, including the development of spontaneous neuronal activity [10] and synchronized bursting [11]. It has also been shown that these networks are responsive to neurotransmitters [12], indicating the presence of a wide range of common neurotransmitter receptors. This technique offers consistent reproducibility across different laboratories [13, 14] and a high sensitivity and specificity [15, 16]. For these reasons mwMEAs are seen as a suitable and consistent in vitro neurotoxicity screening method. Because measurements take place in a sterile environment, this technique allows for both acute [17–19] and chronic toxicity screening [20]. Most mwMEA research was done with rat primary cortical cultures [21–24], but

recently it has been shown that also hiPSC co-cultures grow on mwMEA plates, develop spontaneous activity and bursting behavior, and are suitable for neurotoxicity screening [25–27].

2 Materials

2.1 Cell Culture

For all techniques described in this chapter, we used commercially available hiPSC-derived neurons (iCell® Neurons and iCell® Glutaneurons) and astrocytes (iCell® Astrocytes). All cells were obtained from Cellular Dynamics International (Madison, WI, USA). Cells were cultured at 37 °C in a humidified 5% CO_2 incubator. From previous experiments, we know that these cells grow better on polyethylenimine (PEI)-coated surfaces compared to poly-L-lysine (PLL)- or poly-L-ornithine (PLO)-coated materials. We therefore pre-coated all our cell culture surfaces with 0.1% PEI solution diluted in borate buffer (24 mM sodium borate/50 mM boric acid in Milli-Q, pH adjusted to 8.4) unless stated otherwise. Co-cultures were grown in BrainPhys™ medium supplemented with 2% iCell Neuron supplement, 1% nervous system supplement, 1% penicillin-streptomycin, 1% N2 supplement, and 0.1% laminin (L2020 Sigma-Aldrich, Zwijndrecht, The Netherlands). Astrocytes (iCell®) were cultured in astrocyte medium (DMEM with high glucose and 10% FBS, 1% N2 supplement, and 1% penicillin-streptomycin).

Young astrocytes can proliferate rapidly and potentially overgrow neuronal cultures. Astrocytes were therefore passaged two to three times and stored in liquid nitrogen until use in co-culture with the hiPSC-derived neurons. Young astrocytes were thawed by gently swirling them for 2–3 min in a 37 °C water bath. Then, the content of the vial was transferred to a sterile 50 mL tube. The vial was rinsed three times with astrocyte medium. Total volume in the 50 mL tube was brought to 10 mL, and cells were centrifuged for 5 min at 1300 rpm. The cell pellet was dissolved in 6 mL astrocyte medium, and cells were transferred to a 25 cm^3 Geltrex™-coated culture flask (Geltrex™ was added to cover the bottom of the flask and incubated for 45–60 min at 37 °C in a humidified incubator, after which the Geltrex™ was removed). These flasks were used for a total of 1–1.4 × 10^6 cells. Astrocyte medium was replaced every 3–4 days. Cells were passaged by removing the medium, rinsing with PBS and adding 1 mL 0.0125% trypsin for ~5 min to the flask. During trypsin incubation the flask was placed at 37 °C in a humidified 5% CO_2 incubator. It is important to carefully check that cells are detached since astrocytes adhere strongly to the flask and may require more than 5 min incubation. Once the cells were detached, 9 mL of medium was added to the cells. Cells were counted and centrifuged for 5 min at 1300 rpm. For passaging, 3–4.2 × 10^6 cells were transferred to a 75 cm^3 Geltrex™-coated culture flask, and the volume was brought to 20 mL. In case cells

were used for co-culturing and not for passaging, the cell pellet was dissolved in Complete iCell Neurons Maintenance Medium supplemented with 1% penicillin-streptomycin, 2% iCell Neuron medium supplement, and 1% laminin (L2020, Sigma-Aldrich, Zwijndrecht, The Netherlands) into a 14,000 cells/μL solution.

Procedures for thawing of iCell® Neurons and iCell® Glutaneurons are comparable. The vial with neurons was thawed by gently swirling it for 2–3 min in a 37 °C water bath. The cell suspension was transferred to a 50 mL tube, and the vial was rinsed three times with Complete iCell Neurons Maintenance Medium. The total volume in the 50 mL tube was brought to 10 mL, and the tube was turned upside down twice. A sample for cell counting was taken, and cells were centrifuged for 5 min at 1300 rpm. The pellet of iCell® Neurons was dissolved in dotting medium (i.e., supplemented BrainPhys™ medium with 10% laminin) to a solution of 14,000 cells/μL. In parallel, iCell® Glutaneurons were dissolved in dotting medium to a solution of 13,000 cells/μL.

When all cells were thawed or detached, we created two types of co-culture models that differ in the ratio of inhibitory neurons by addition or absence of iCell® Neurons to create different profiles of neuronal activity (see [25] for details). First, a mixture was made of ~13% iCell® Astrocytes, ~17% iCell® Neurons, and ~70% iCell® Glutaneurons (culture model A) according to Table 1. Cells were plated in 10 μL droplets (Table 2). In order to get the total

Table 1
Composition of cell models and plating density

Culture	Cell type and %	N/well	Solution	μL/well
A	~13% astrocytes	10,000	14,000 cells/μL	0.71 μL
	~17% iCell® Neurons	13,000	14,000 cells/μL	0.93 μL
	~70% iCell® Glutaneurons	52,000	13,000 cells/μL	4 μL
B	~15% astrocytes	11,250	14,000 cells/μL	0.80 μL
	~85% iCell® Glutaneurons	63,750	13,000 cells/μL	4.55 μL

Table 2
Cell culture surfaces and medium volume

Culture surface	Experiment	Total volume
48-well MEA plate (Axion Biosystems Inc., Atlanta, GA, USA)	MEA recording	300 μL/well
μ-slide 8-well chambered coverslip (ibidi GmbH, Planegg, Germany)	Immunocytochemistry	200 μL/well
Glass-bottom dishes (MatTek, Ashland MA, USA)	Live fluorescence imaging	2 mL/dish

volume to 10 µL, 4.36 µL dotting medium was added. For culture model B, a mixture was made of ~15% iCell® Astrocytes and ~85% iCell® Glutaneurons (according to Table 1). In this case, 4.65 µL dotting medium was added to bring the total plating volume to 10 µL. Following plating, droplets were allowed to adhere for 1 h after which medium was added (Table 2). On DIV1, 50% of the medium was refreshed with room temperature (RT) supplemented BrainPhys™ medium. Hereafter, 50% medium changes took place three times a week up till DIV23.

Since both co-culture models require several days to develop functional neuronal networks, MEA and imaging experiments should not be performed before DIV11. In our experience, the optimum window for performing MEA and live imaging experiments ranges from DIV14 to DIV23. It should be noted that the optimum window for measurements differs between the various available commercial models as well as culture conditions (e.g., cell density and % astrocytes).

It should be noted that using a high ratio of astrocytes may cause the cells to cluster, complicating imaging and MEA experiments. Developmental curves can be measured from DIV4 onward and can be used to determine the optimum window for assessing acute neurotoxicity. We strongly recommend to always measure a developmental curve before performing neurotoxicity assessment when starting to work with new cells and/or new culture protocols.

2.2 Confocal Microscopy for Immunocytochemistry

Immunofluorescent images of chemically fixed samples were captured with a Leica DMI4000 TCS SPEII confocal microscope. To capture images, a 20× oil immersion objective (ACS APO IMM NA 0.6) was used. The 20× objective allows for visualization of multiple neurons in one frame with the connecting dendrites and axons being clearly visible. When a 10× objective is used, too many details and sensitivity are lost, whereas a 40× objective does not capture the complexity of the network structure. It is recommended to visually scan the complete chamber to make sure the selected area is representative for the culture. We noticed that the neuronal co-cultures tend to grow differently at the periphery of the culture area compared to the center. In order to capture an area that best matches the region where MEA measurements take place, a region in the middle of the dish is chosen. Once a representative area is found, it's recommended to define an upper and lower limit in order to make a picture based on *z-stacks*. We recommend imaging a *z-stack* series, since the elaborate extensions of the cells are poorly captured in a single plane. An axially extended view provided by a maximal intensity projection visualizes the structures better. Images were captured as .lif files using Leica Application Suite Advanced Fluorescence software (LAS AF version 2.6.0; Leica Microsystems GmbH, Wetzlar, Germany).

2.3 Live Cell $[Ca^{2+}]_i$ Changes Using a Temperature Controlled Microscopy Unit

Live changes in $[Ca^{2+}]_i$ were monitored with the fluorescent dye Fura-2AM (Ex 340 and 380/Em 510, Life Technologies, Bleiswijk, The Netherlands) using an Axiovert 35 M inverted microscope (Zeiss, Göttingen, Germany) as described previously [28]. We used a 40× oil immersion objective (Plan-NeoFluar NA 1.30) to capture images. Light with an excitation wavelength of 340 and 380 nm evoked by a monochromator (TILL Photonics Polychrome IV; TILL Photonics GmBH, Gräfelfing, Germany) was directed to the sample via a 290 nm long-pass filter and beam splitter. From there, the emitted light with a wavelength of 510 nm was directed to a 440 nm long-pass filter and was collected every 0.5 s, i.e., at a sample frequency of 2 Hz for each excitation wavelength, with an Image SensiCam digital camera (TILL photonics GmBH). The degree of fluorescence in Fura-2-loaded neuronal co-cultures allowed us to sample with binning 2 × 2. TILLvisION (version 4.01) software was used to trigger the light source, camera, and data acquisition.

For the cells to exhibit spontaneous network activity, experiments must take place at 37 °C. Below this temperature no spontaneous calcium oscillations are visible (data not shown). In order to keep our samples at a stable temperature, we equipped the microscope with a custom-built heating system and bipolar temperature control unit (TC-202, Medical Systems Corp, Greenvale, New York, USA).

Changes in the ratio F340/F380 of selected regions of interest reflecting the changes in $[Ca^{2+}]_i$ were further analyzed using custom-made MS Excel macros. Since the cells form networks, spontaneous synchronous calcium oscillations are seen in all regions.

2.4 Simultaneous Live Cell Imaging of Calcium Transients and Membrane Depolarization

To monitor calcium levels, X-Rhod-1 (Ex 580/Em 602, AM-ester derivative, Life Technologies, Bleiswijk, The Netherlands) was used and for membrane depolarization the dye FluoVolt (Ex 488/Em 515, Life Technologies, Bleiswijk, The Netherlands).

Live cell microscopic fluorescence recordings were performed on a commercial NIKON Ti system equipped with an EMCCD camera (iXon Ultra897, ANDOR) using wide-field illumination. A 10× CFI Plan Fluor air objective (NA 0.3, WD 16 mm) was applied to record the data. A LED light source (Lumencor Spectra X) illuminated the samples to deliver 470/24 nm and 575/25 nm light bandwidths sequentially. Emitted fluorescence light was collected through a quadband emission filter (Chroma, DAPI/FITC/TRITC/Cy5 Quad). Triggered synchronization of the LEDs and the camera was directed with the NIS-Elements software ND acquisition module (NIKON, version 4.6) via a NIDAQ communication board (National Instruments). Halogen illumination light path was regulated by a fast shutter (Lambda SC, SUTTER Instruments) to obtain differential interference contrast (DIC)

images without the delay of slow on and off glowing rates of these lamps. Fast focus control is performed by a piezo stepping stage device (Mad City Labs, Madison, WI, USA).

In the Spectra X module of the NIS-Elements software, the 470 nm and 575 nm light sources were controlled. Via the triggered acquisition module, light levels and exposure times were set (<3%, ND4 and eight filters were available for careful illumination modulation). The EMCCD camera capture area was cropped to 256 × 256, and 2 × 2 binning was applied at 20 ms exposures (sampling in frame transfer mode at 17 Mhz horizontal pixel shift readout frequency with 300 V amplification gain).

The system is equipped with temperature and CO_2 control in a stage top setup with a small water container to provide a humidified culture environment (TOKAI HIT, INUBG2EH-TiZB). The lens heating option was omitted for the air objectives employed.

Both the automated focus control system of NIKON (perfect focus system or pfs) and the compressor that provides air for the vibration isolation table can create vibrations and were thus switched off for the recordings.

Following data acquisition, recorded data was exported to MS Excel. For further frequency data analysis, one representative trace from a dish was chosen as all cells display synchronized oscillations in calcium levels and membrane potential. To calculate changes in peak amplitude, data was loaded in a custom-made MATLAB program, and averages of multiple responsive cells in the dish were calculated. Data are reported as mean ± SEM form n cells.

2.5 Multi-well Microelectrode Array Recordings

Cells were cultured on 48-well MEA plates (Fig. 1) as described previously [12, 17]. Each well contains an electrode array of 16 nanotextured gold microelectrodes that are ~40–50 μm in diameter with a 350 μm center-to-center spacing. Each well contains four integrated ground electrodes. In total this yields 768 channels in one plate that can be recorded simultaneously. A Maestro 768-channel amplifier with an integrated heating system, temperature controller, and data acquisition interface (Axion Biosystems Inc., Atlanta, GA, USA) was used for recordings of neuronal activity. Data acquisition was managed with Axion's Integrated Studio (AxIS version 2.4.2.13) and recorded as .RAW files. Files were obtained by sampling all channels simultaneously with a gain of 1200× and a sampling frequency of 12.5 kHz/channel using a band-pass filter (200–5000 Hz). Notably, the large number of electrodes, sampled at high frequency, will yield a large amount of data (~1 GB/min recording). Consequently, sufficient storage space should be available.

For data analysis .RAW files were re-recorded to obtain alpha map files. During this re-recording, spikes were detected using the AxIS spike detector (adaptive threshold crossing, Ada BandFIt v2). A variable threshold spike detector was used with a threshold set at

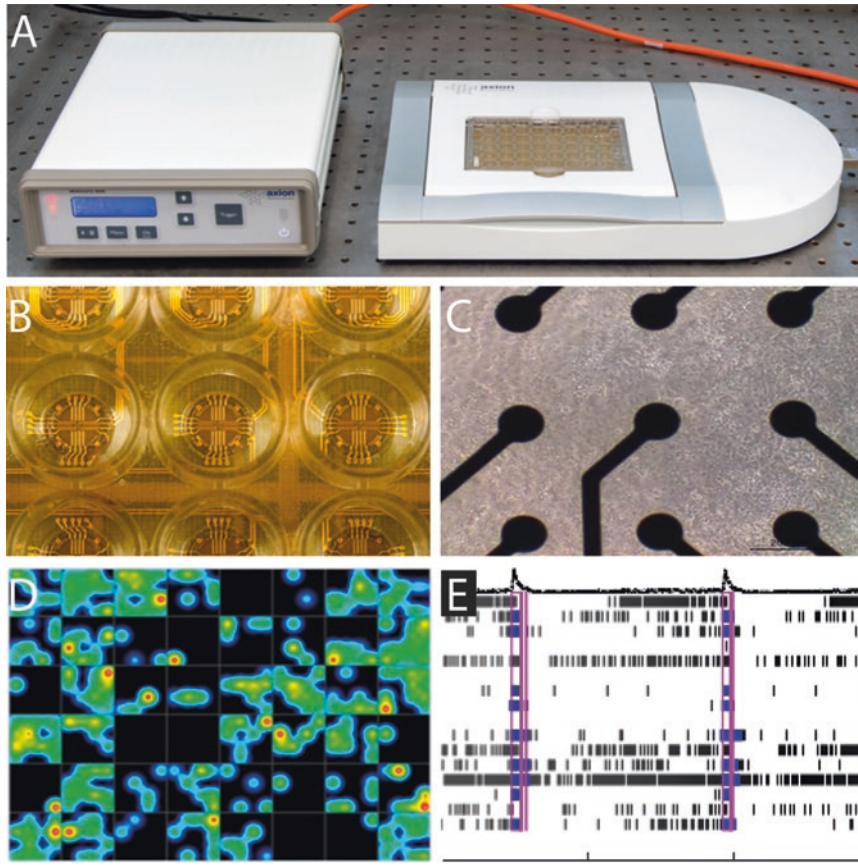

Fig. 1 Experimental setup for measurements of spontaneous neuronal network activity. Axion's Maestro platform (**a**) was used to record neuronal activity of co-cultures grown in 48-well MEA plates (**b**). Each well contains an electrode grid with 16 electrodes/well (**c**) for noninvasive extracellular field recordings. Live heat maps are shown in AxIS software during recordings (**d**). Files are loaded in neural metric to determine (**e**) spikes (black), bursts (blue), and network bursts (pink squares)

7× standard deviation of the internal noise level (rms) on each electrode. The obtained spike files were loaded in Neural Metric (version 2.04, Axion Biosystems). In this program, bursts were detected with the Poisson surprise method (minimal surprise $S = 10$ [29]). Network bursts were extracted with the adaptive threshold method (min # of spikes 10; min % of electrodes 25).

The Neural Metric output files (.csv files) were loaded in a custom-made MS Excel macro. We only used active electrodes (MSR ≥ 6 spikes/min) from active wells (≥1 active electrode) for further analysis. Electrodes were seen as bursting electrodes when the minimum burst rate was ≥0.001 bursts/s. Only wells with ≥2 bursting electrodes were included for network bursting and synchronicity analysis. Effects of test compounds were determined by comparing the activity of the baseline of a well to the activity in that well following exposure. During data analysis it is important to

correct for exposure artifacts [12]. To do so, the time it took to expose all wells was excluded from data analysis. For example, if exposing the plate took 2 min, the first 2 min of the recording was not used for data analysis but only the subsequent 30 min. Then, treatment ratios per well for different metric parameters (mean spike rate [MSR], mean burst rate [MBR], and mean network burst rate [MNBR]) were calculated by expressing the $\text{parameter}_{\text{exposure}}$ as a percentage change of $\text{parameter}_{\text{baseline}}$. Next, treatment ratios were normalized to vehicle control. Outliers were defined as not within average ± 2× standard deviation and excluded for further analysis. MEA data are expressed as mean ± SEM. A one-way ANOVA was performed to determine statistical significant changes ($p < 0.05$) in MSR, MBR, and MNBR compared to vehicle control.

3 Methods and Results

3.1 Immunocytochemistry: Visualizing Neuronal Networks

Neuronal networks of culture model A were chemically fixed, and specific antibodies were used to demonstrate the presence of neurons and astrocytes. Neurons were identified using antibodies against class III β-tubulin, which is found almost exclusively in neurons. Anti-s100β is a protein specific for glial cells and was used to identify astrocytes. Notably, many other antibodies can be used to gain additional insight in the composition of the neuronal network. For example, using antibodies against vGLUT (vesicular glutamate transporter), vGAT (vesicular GABA transporter), or tyrosine hydroxylase (marker for dopaminergic neurons) will provide information on the types of neurons present.

In order to stain the cultures, a staining protocol described previously [25] was used. The cultures were chemically fixed at DIV16 and 21 with 4% PFA in 0.1 M PBS (pH 7.4) for 15 min at RT. We found that longer fixation times reduced epitope recognition by the antibodies. Following fixation, chambered coverslips were quenched for PFA, permeabilized, and incubated for 20 min at RT with 20 mM NH_4Cl in blocking buffer (2% bovine serum albumin and 0.1% saponin in PBS). Hereafter, chambers were incubated overnight at 4 °C with the primary antibody. The following primary antibodies were used: mouse anti-S100β (final dilution 1:500; Ab11178, Abcam, Cambridge, United Kingdom) to stain astrocytes and rabbit anti-βIII tubulin (final dilution 1:250; Ab18207, Abcam, Cambridge United Kingdom) to visualize the iCell® Neurons and iCell® Glutaneurons. The following day, chambers were washed thrice with blocking buffer and incubated with donkey anti-rabbit Alexa Fluor® 488 (final dilution 1:100; 715-545-152, Life Technologies, Bleiswijk, The Netherlands) and donkey anti-mouse Alexa Fluor® 594 (final dilution 1:100; 715-585-151, Life Technologies, Bleiswijk, The Netherlands) for 45 min at RT in the dark. During the last 2–3 min of the incubation time, 200 nM DAPI (staining the nuclei) was added. Chambers

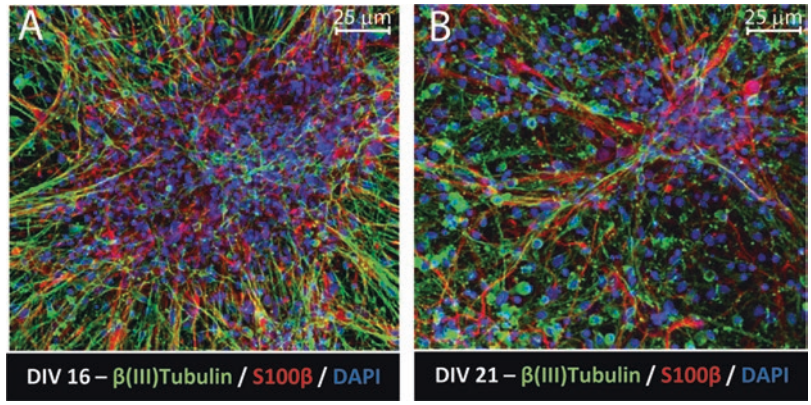

Fig. 2 Immunofluorescent stainings of co-culture model A. At DIV16 (**a**) and DIV21 (**b**), cultures were stained with β(III) tubulin (green) and S100β (red) to identify, respectively, neurons and astrocytes in the co-culture. Nuclei were stained with DAPI (blue). Scale bar depicts 25 μm

were washed again 3× with blocking buffer and sealed with two to three droplets of FluorSave (Calbiochem, San Diego, CA, USA). Now the chambers are ready for use. However, they can be stored for months at 4 °C in the dark until use.

The images of the chemically fixed and stained co-cultures of culture model A show that mixed neuronal networks with a high degree of complexity are formed (Fig. 2a, b). It is clear that the network is already strongly developed at DIV16 (Fig. 2a) and this is maintained till DIV21 (Fig. 2b). The images also show that astrocytes do not overgrow the neuronal population. The ratio astrocytes to neurons remains comparable over time and is in line with the plated ratio. Altogether, these results indicate that this co-culture consists of a mixed cell population with neurons as well as supporting astrocytes that can be used for neurotoxicity testing.

3.2 Live Cell Imaging: $[Ca^{2+}]_i$ Changes in hiPSC-Derived Co-cultures

Both dyes used for the $[Ca^{2+}]_i$ experiments described in this chapter contain an acetoxymethyl (AM) ester. The AM group allows the dye to cross the cell membrane, which allows the cells to be loaded in a noninvasive manner. Following membrane crossing, the AM group is cleaved from the dye by non-specific esterases in the cytosol. The cleaved dye is no longer able to cross the cell membrane and remains in the cytosol. The calcium-sensitive dye Fura-2 is fluorescent green (510 nm), and fluorescence increases upon Ca^{2+} binding following excitation at 340 nm, but fluorescence decreases by excitation at 380 nm. The resulting F340/380 ratio thus correlates directly with the $[Ca^{2+}]_i$.

Cells cultured in glass-bottom dishes of culture model B were loaded with 5 μM Fura-2AM for 1 h at 37 °C in a humidified 5% CO_2 incubator. After loading, cells were washed four times with 37 °C saline solution to remove excess dye. Then dishes with loaded cells were placed on the stage of the inverted microscope in the heating ring. The temperature sensor was placed in the dish,

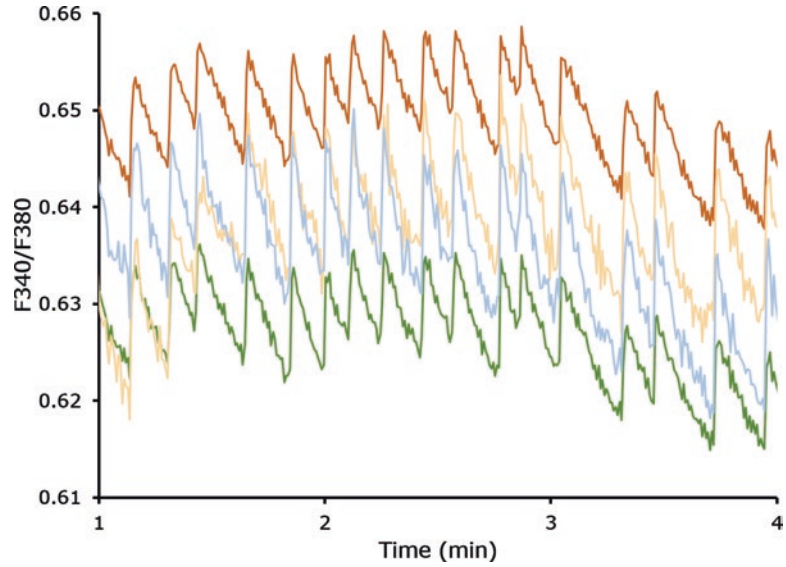

Fig. 3 Sample traces of representative neuronal cells (DIV23) showing spontaneous calcium oscillations. Each trace represents the oscillations of a single cell over a 3 min time period. Cells oscillate synchronously, indicating they are part of a single network

and cells were allowed to warm till 37 °C. As soon as this temperature was reached, a 5 min recording was started to measure spontaneous calcium oscillations.

With this method it is possible to detect spontaneous calcium oscillations in hiPSC-derived neuronal co-cultures (Fig. 3). Sample traces indicate the presence of spontaneous calcium oscillations. Cells oscillate synchronously, indicating that cells are all part of a single network.

3.3 Live Cell Imaging: Simultaneous Calcium Oscillations and Membrane Depolarization in hiPSC-Derived Co-cultures

X-rhodamine-1 (X-RhodAM) was used to study spontaneous calcium oscillations. This dye works in a comparable manner as Fura-2AM. However, the main difference is that Fura-2AM is a dual wavelength dye and X-RhodAM a single wavelength dye in the red color range (emission 595 nm). The latter has as advantage that it can be imaged at a higher sample frequency and allowing it to be used in combination with other sensor dyes. In order to study simultaneous changes in membrane depolarization, we used the dye FluoVolt. In general there are two types of probes that can be used to do this: fast- or slow-response probes. The first type reacts fast, but the magnitude of potential-dependent fluorescence change is small. The latter type reacts slower, but the magnitude of fluorescence fluctuation is high. FluoVolt is a dye that combines characteristics of fast and slow probes as it reacts fast (millisecond time scale) and yields a high magnitude of fluorescence with a small change in membrane potential (~25% change in fluorescence per 100 mV change in membrane potential).

Cells of culture model B were cultured up till DIV21 in glass-bottom dishes and used to record changes in calcium transients and membrane voltage fluctuations. One day prior to measurements, cells were transferred to an incubator close to the imaging station to minimize transport stress and temperature variation at the time of the experiment. At the day of measurements, start the microscope peripheral modules (Spectra X, Mad City Labs stage control, XY control joystick unit, halogen lamp, and TOKAI HIT control unit) before powering the microscope stand and finally turn on the PC. Distilled water was placed in the basin of the TOKAI HIT sample holder. It is important to place a dummy sample in the holder to prevent condensation on optics below the table. At this point, the climate control unit (37 °C for the basin, 40 °C for the TOP deck heating, 5% CO_2) is switched on, and the whole setup is left for acclimatization for 30 min. All experiments took place at 37 °C.

During the acclimatization time, cultures were loaded with a mixture of 5 μM X-Rhod-1, 5 μM FluoVolt, and PowerLoad solution (a solubilizing agent provided in FluoVolt kit) in life cell imaging solution (LCIS; 140 mM NaCl, 2.5 mM KCl, 1.8 mM $CaCl_2$, 1.0 mM $MgCl_2$, 20 mM HEPES, 20 mM glucose) for 15–20 min. Following incubation, cells were washed four times with 1 mL LCIS. After loading, the sample was placed in the TOKAI HIT holder (UNIVD35) to search for a representative area and select regions of interest (ROIs) to obtain live intensity preview plots (Fig. 4). Next, a 10 min baseline recording was made prior to addition of test compound and a subsequent 10 min exposure recording. For exposure recordings, a fresh stock solution of picrotoxin (PTX) in EtOH was prepared on the day of the experiment. Stock solution was further diluted in LCIS. Solvent concentration did not exceed 0.1% v/v.

Data again confirm that neuronal co-cultures form networks, since oscillations in membrane potential as well as calcium occur for all cells at the same time (Fig. 5a, b left). Exposure (dilution

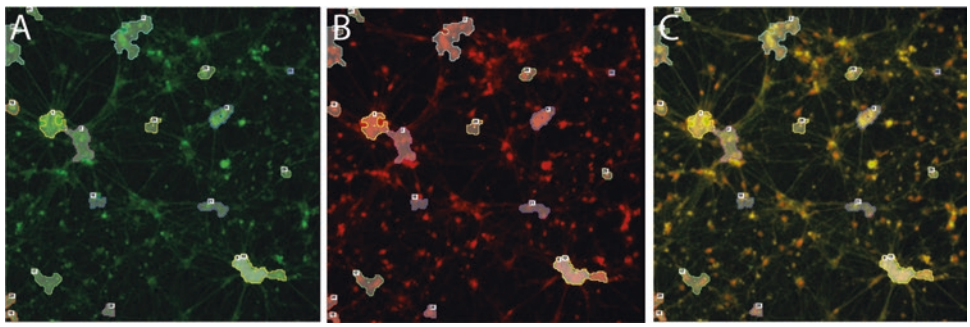

Fig. 4 Captures of neuronal cells loaded with FluoVolt (**a**), X-Rhod (**b**), and an overlay (**c**). Encircled areas are selected regions of interest for measurements as further illustrated in Fig. 5

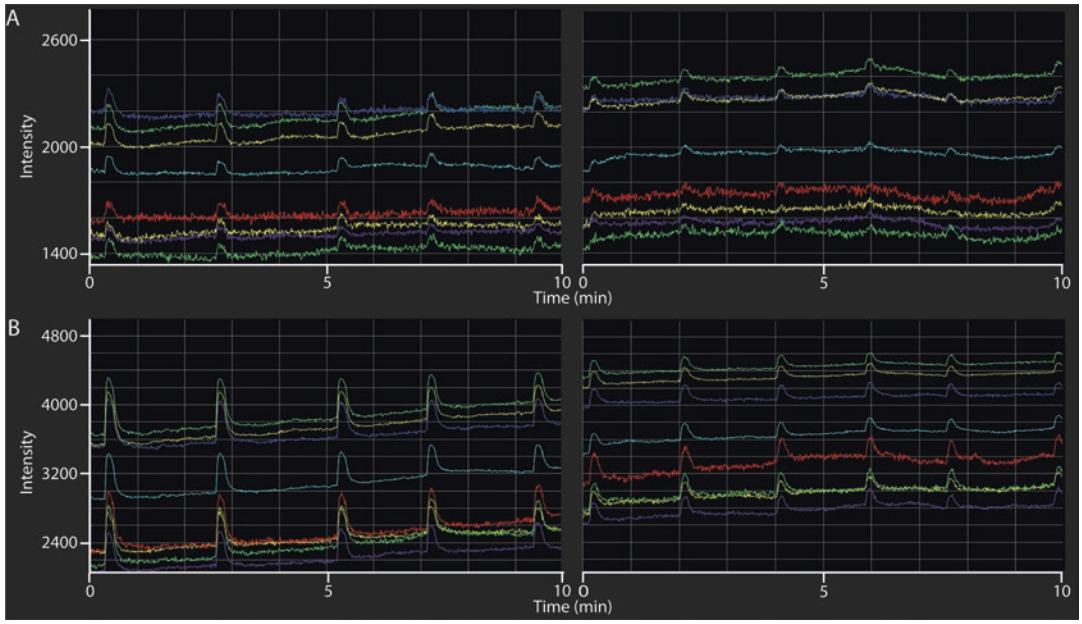

Fig. 5 Selection of traces of cells selected in Fig. 4 for assessing changes in fluorescence of FluoVolt (**a**) and X-Rhod-1 (**b**) during baseline (left) and exposure (right) to 10 **μ**M PTX. Different cells oscillate simultaneously, indicating that changes in membrane potential (**a**) and $[Ca^{2+}]_i$ (**b**) occur at the same time and the cells are part of the same neuronal network

1:10) to 10 μM (PTX) does not affect the frequency of oscillations. However, it does result in a decrease of the amplitude of membrane potential peaks to 57.2% (±3.4, $n = 6$) of baseline (Fig. 5a). A stronger effect is seen on calcium oscillations, where amplitude decreases to 37.5% (±3.2, $n = 6$) compared to baseline (Fig. 5b). Basal fluorescence increases over time, likely as a result of ongoing de-esterification of dye that still contained the AM module. However, filter and/or subtraction methods can be used to eliminate this trend in fluorescence from data analysis.

3.4 MEA: Assessing Spontaneous Neuronal Network Activity in hiPSC-Derived Co-cultures

All MEA measurements took place at 37 °C with culture model B. Experiments took place at DIV21 since this is the optimum window in terms of activity (Table 3). It should be noted that different culture models develop differently and may therefore have a different optimum window. For this reason, it is strongly recommended to always make a developmental curve before starting toxicity experiments. In order to determine effects of test compounds on spontaneous network activity and (network) bursting of the hiPSC-derived co-culture, a 30 min baseline recording was made. Prior to the 30 min recording, plates were allowed to equilibrate in the Maestro for ~5 min. Immediately following this 30 min baseline recording, cells were exposed (dilution 1:10) to the test compounds or the solvent control, and another 30 min recording was made. Each well was exposed only once, since cumulative dosing

Table 3
Development of spontaneous neuronal activity and (network) bursting at different DIVs. Data are expressed as mean ± SEM

	MSR		MBR		MNBR	
	Frequency (Hz)	% active wells	Frequency (Hz)	% active wells	Frequency (Hz)	% active wells
DIV7	1.53 ± 0.14	93.8	0.04 ± 0.01	26.7	0.01 ± 0.01	25
DIV14	1.43 ± 0.14	93.8	0.02 ± 0	13.3	0.01 ± 0.01	100
DIV21	1.29 ± 0.18	93.8	0.05 ± 0.01	76.7	0.03 ± 0.03	65.2

may confound results due to, e.g., receptor (de)sensitization. We prepared fresh PTX stock solutions in EtOH and of strychnine in supplemented BrainPhys™ medium prior to every experiment. Stock solutions of PTX were further diluted in supplemented BrainPhys™ medium such that solvent concentration never exceeded 0.1% v/v.

Neuronal activity in culture model B can be modulated with strychnine (Fig. 6a). Exposure to the highest tested concentration strongly decreases MSR, MBR, and MNBR (Fig. 6a, right) as compared to baseline activity (Fig. 6a, left). The inhibitory effect of strychnine on MSR is concentration-dependent (Fig. 6b). This in contrast to the MBR, which increases following exposure to low concentrations of strychnine and decreases following exposure to higher concentrations. MNBR decreases by all tested concentrations of strychnine. Exposure to PTX (Fig. 6b) has little effect on the MSR, except for exposure to 1 μM, which decreases the MSR. The lowest test concentration of PTX causes a decrease in MBR; however with increasing concentrations, the MBR increases as well. On the other hand, all tested concentrations of PTX cause a decrease in MNBR.

The different effects that strychnine and PTX have on culture model B become clear from the inclusion of additional metric parameters illustrated by a heat map (Fig. 7). This heat map also indicates that for proper MEA data analysis, it is important to include more parameters than just MSR, MBR, and MNBR.

4 Conclusions

Human iPSC-derived co-cultures develop functional and spontaneously active neuronal networks consisting of mature neurons [8, 30]. Our immunocytochemistry data demonstrate the mixed nature of our co-culture models consisting of neurons and astrocytes that form complex, multicellular networks (Fig. 2).

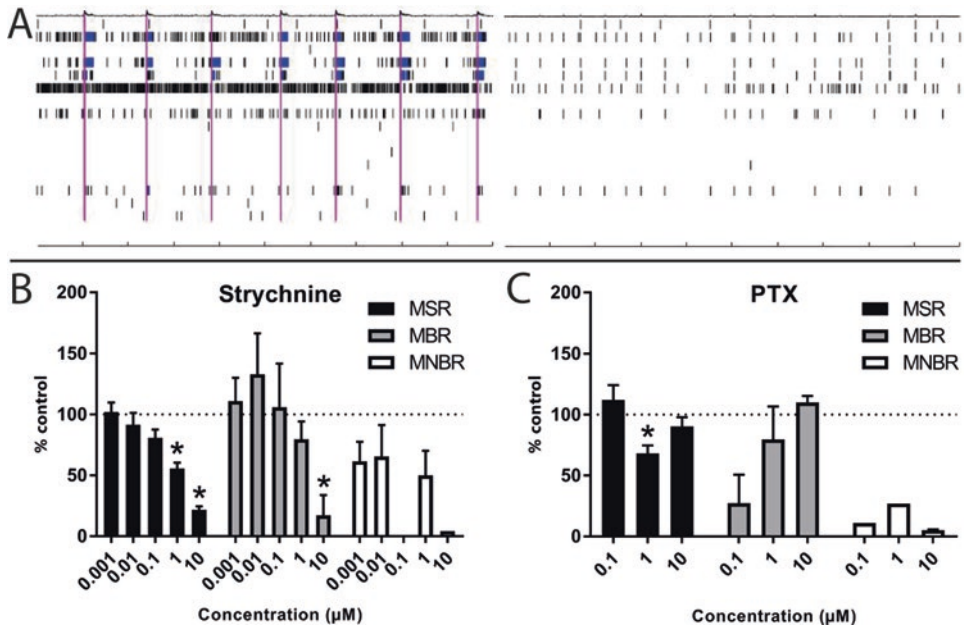

Fig. 6 Toxicological modulation of spontaneous network activity, bursting, and network bursting. Cultures were exposed at DIV21 to strychnine (**a**, **b**) or PTX (**c**). Spike raster plot depicting activity and (network) bursting before (left) and following exposure (right) to 10 µM strychnine (**a**). Each row depicts one electrode, each tick representing one spike (field potential) in a 200 s interval, bursts are depicted in blue, and network bursts are encircled in pink squares. Data are expressed as MSR, MBR, or MNBR as % change relative to vehicle control; mean ± SEM from $n = 1–12$; $^*p < 0.05$ (**b**, **c**)

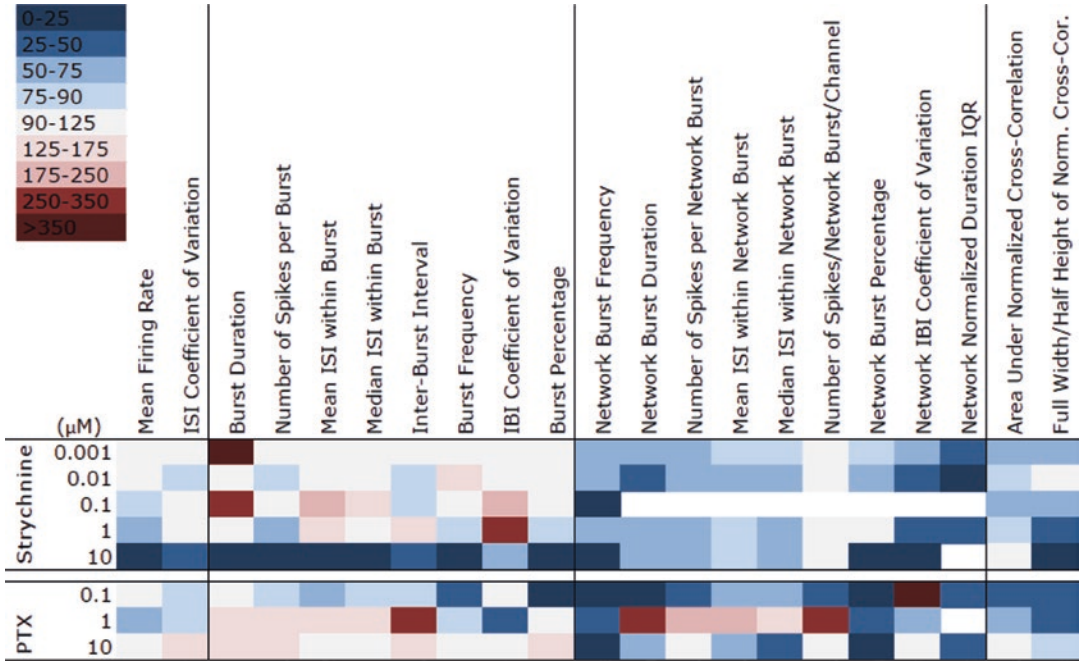

Fig. 7 Heat map of the effects of strychnine and PTX (concentration in µM) on selected metric parameters on culture model B. Color scaling is based on the magnitude of the % of change relative to the vehicle control. No average could be calculated for white cells

We have shown that hiPSC-derived neuronal co-cultures are amenable to multiple real-time recording techniques, including live cell imaging and electrophysiology. Our calcium imaging data indicate that the co-culture models develop spontaneous calcium oscillations and spontaneous changes in membrane potential (Figs. 3 and 5). Since calcium oscillations and changes in membrane potential occur in multiple cells at the same time (Figs. 3 and 5), it can be concluded that functional networks are formed. Moreover, MEA recordings demonstrate that neuronal co-cultures develop spontaneous network activity and (network) bursting (Table 3 and Fig. 6).

Spontaneously active human iPSC-derived neuronal co-cultures are suitable for (preliminary) neurotoxicity assessment [18, 25, 27, 31, 32] as is confirmed by our data (Figs. 5, 6, and 7). However, it must be noted that model composition, e.g., the ratio of GABAergic and glutamatergic neurons and the presence of astrocytes, greatly influences the model's characteristics [25]. Therefore, a careful model characterization must be performed prior to toxicity testing.

The increasing availability of hiPSC from different donors and/or patients differentiated in different cell types, e.g., GABAergic, glutamatergic, dopaminergic neurons and astrocytes as well as peripheral neurons, holds great promise for future personalized toxicity and safety screening. Using hiPSC-derived neurons in combination with the techniques described here will provide a good starting point for neurotoxicity assessment.

Acknowledgments

We gratefully acknowledge members of the Neurotoxicology Research Group for helpful discussions. This work was funded by a grant from the National Centre for the Replacement, Refinement and Reduction of Animals in Research (NC3Rs; project number 50308-372160), the Netherlands Organisation for Health Research and Development (ZonMW; InnoSysTox project number 114027001), and the Faculty of Veterinary Medicine (Utrecht University, The Netherlands).

References

1. Clapham DE (2007) Calcium signaling. Cell 131:1047–1058. https://doi.org/10.1016/J.CELL.2007.11.028
2. Westerink R (2006) Targeting exocytosis: ins and outs of the modulation of quantal dopamine release. CNS Neurol Disord Drug Targets 5:57–77. https://doi.org/10.2174/1871527067841115 97
3. Barclay JW, Morgan A, Burgoyne RD (2005) Calcium-dependent regulation of exocytosis. Cell Calcium 38:343–353
4. Südhof TC (2014) The molecular machinery of neurotransmitter release (nobel lecture). Angew Chem Int Ed 53:12696–12717. https://doi.org/10.1002/anie.201406359

5. Kuijlaars J, Oyelami T, Diels A et al (2016) Sustained synchronized neuronal network activity in a human astrocyte co-culture system. Sci Rep 6:36529. https://doi.org/10.1038/srep36529
6. Görtz P, Fleischer W, Rosenbaum C et al (2004) Neuronal network properties of human teratocarcinoma cell line-derived neurons. Brain Res 1018:18–25. https://doi.org/10.1016/j.brainres.2004.05.076
7. Odawara A, Katoh H, Matsuda N, Suzuki I (2016) Physiological maturation and drug responses of human induced pluripotent stem cell-derived cortical neuronal networks in long-term culture. Sci Rep 6:26181. https://doi.org/10.1038/srep26181
8. Paavilainen T, Pelkonen A, Mäkinen ME-L et al (2018) Effect of prolonged differentiation on functional maturation of human pluripotent stem cell-derived neuronal cultures. Stem Cell Res 27:151–161. https://doi.org/10.1016/j.scr.2018.01.018
9. Johnstone AFM, Gross GW, Weiss DG et al (2010) Microelectrode arrays: a physiologically based neurotoxicity testing platform for the 21st century. Neurotoxicology 31:331–350
10. Robinette BL, Harrill JA, Mundy WR, Shafer TJ (2011) In vitro assessment of developmental neurotoxicity: use of microelectrode arrays to measure functional changes in neuronal network ontogeny1. Front Neuroeng 4:1. https://doi.org/10.3389/fneng.2011.00001
11. Cotterill E, Hall D, Wallace K et al (2016) Characterization of early cortical neural network development in multiwell microelectrode array plates. J Biomol Screen 21:510–519. https://doi.org/10.1177/1087057116640520
12. Hondebrink L, Verboven AHA, Drega WS et al (2016) Neurotoxicity screening of (illicit) drugs using novel methods for analysis of microelectrode array (MEA) recordings. Neurotoxicology 55:1–9. https://doi.org/10.1016/j.neuro.2016.04.020
13. Novellino A, Scelfo B, Palosaari T et al (2011) Development of micro-electrode array based tests for neurotoxicity: assessment of interlaboratory reproducibility with neuroactive chemicals. Front Neuroeng 4:4. https://doi.org/10.3389/fneng.2011.00004
14. Vassallo A, Chiappalone M, De Camargos Lopes R et al (2017) A multi-laboratory evaluation of microelectrode array-based measurements of neural network activity for acute neurotoxicity testing. Neurotoxicology 60:280–292. https://doi.org/10.1016/j.neuro.2016.03.019
15. McConnell ER, McClain MA, Ross J et al (2012) Evaluation of multi-well microelectrode arrays for neurotoxicity screening using a chemical training set. Neurotoxicology 33:1048–1057. https://doi.org/10.1016/j.neuro.2012.05.001
16. Valdivia P, Martin M, LeFew WR et al (2014) Multi-well microelectrode array recordings detect neuroactivity of ToxCast compounds. Neurotoxicology 44:204–217. https://doi.org/10.1016/j.neuro.2014.06.012
17. Nicolas J, Hendriksen PJM, van Kleef RGDM et al (2014) Detection of marine neurotoxins in food safety testing using a multielectrode array. Mol Nutr Food Res 58:2369–2378. https://doi.org/10.1002/mnfr.201400479
18. Hondebrink L, Kasteel EEJ, Tukker AM et al (2017) Neuropharmacological characterization of the new psychoactive substance methoxetamine. Neuropharmacology 123:1–9. https://doi.org/10.1016/j.neuropharm.2017.04.035
19. Bradley JA, Luithardt HH, Metea MR, Strock CJ (2018) In vitro screening for seizure liability using microelectrode array technology. Toxicol Sci 163:240–253. https://doi.org/10.1093/toxsci/kfy029
20. Dingemans MML, Schütte MG, Wiersma DMM et al (2016) Chronic 14-day exposure to insecticides or methylmercury modulates neuronal activity in primary rat cortical cultures. Neurotoxicology 57:194–202. https://doi.org/10.1016/j.neuro.2016.10.002
21. Hogberg HT, Sobanski T, Novellino A et al (2011) Application of micro-electrode arrays (MEAs) as an emerging technology for developmental neurotoxicity: evaluation of domoic acid-induced effects in primary cultures of rat cortical neurons. Neurotoxicology 32:158–168. https://doi.org/10.1016/j.neuro.2010.10.007
22. Alloisio S, Nobile M, Novellino A (2015) Multiparametric characterisation of neuronal network activity for in vitro agrochemical neurotoxicity assessment. Neurotoxicology 48:152–165. https://doi.org/10.1016/j.neuro.2015.03.013
23. Zwartsen A, Hondebrink L, Westerink RH (2018) Neurotoxicity screening of new psychoactive substances (NPS): effects on neuronal activity in rat cortical cultures using microelectrode arrays (MEA). Neurotoxicology 66:87–97. https://doi.org/10.1016/j.neuro.2018.03.007
24. Frank CL, Brown JP, Wallace K et al (2017) From the cover: developmental neurotoxicants disrupt activity in cortical networks on microelectrode arrays: results of screening 86 com-

pounds during neural network formation. Toxicol Sci 160:121–135. https://doi.org/10.1093/toxsci/kfx169

25. Tukker AM, Wijnolts FMJ, de Groot A, Westerink RHS (2018) Human iPSC-derived neuronal models for in vitro neurotoxicity assessment. Neurotoxicology 67:215–225. https://doi.org/10.1016/J.NEURO.2018.06.007
26. Odawara A, Matsuda N, Ishibashi Y et al (2018) Toxicological evaluation of convulsant and anticonvulsant drugs in human induced pluripotent stem cell-derived cortical neuronal networks using an MEA system. Sci Rep 8:10416. https://doi.org/10.1038/s41598-018-28835-7
27. Tukker AM, De Groot MWGDM, Wijnolts FMJ et al (2016) Is the time right for in vitro neurotoxicity testing using human iPSC-derived neurons? ALTEX 33:261–271. https://doi.org/10.14573/altex.1510091
28. Heusinkveld HJ, Thomas GO, Lamot I et al (2010) Dual actions of lindane (γ-hexachlorocyclohexane) on calcium homeostasis and exocytosis in rat PC12 cells. Toxicol Appl Pharmacol 248:12–19. https://doi.org/10.1016/j.taap.2010.06.013
29. Legéndy CR, Salcman M (1985) Bursts and recurrences of bursts in the spike trains of spontaneously active striate cortex neurons. J Neurophysiol 53:926–939. https://doi.org/10.1152/jn.1985.53.4.926
30. Hyysalo A, Ristola M, Mäkinen MEL et al (2017) Laminin α5 substrates promote survival, network formation and functional development of human pluripotent stem cell-derived neurons in vitro. Stem Cell Res 24:118–127. https://doi.org/10.1016/j.scr.2017.09.002
31. Kasteel EEJ, Westerink RHS (2017) Comparison of the acute inhibitory effects of Tetrodotoxin (TTX) in rat and human neuronal networks for risk assessment purposes. Toxicol Lett 270:12–16. https://doi.org/10.1016/j.toxlet.2017.02.014
32. Ishii MN, Yamamoto K, Shoji M et al (2017) Human induced pluripotent stem cell (hiPSC)-derived neurons respond to convulsant drugs when co-cultured with hiPSC-derived astrocytes. Toxicology 389:130–138. https://doi.org/10.1016/j.tox.2017.06.010